

NPS-57Zi75041

//
NAVAL POSTGRADUATE SCHOOL
Monterey, California



AN EXACT SOLUTION TO THE TRANSONIC EQUATION

by

OSCAR BIBLARZ

APRIL 1975

Approved for public release; distribution unlimited

FEDDOCS
D 208.14/2:NPS-57Zi75041

NAVAL POSTGRADUATE SCHOOL

Monterey, California

Rear Admiral I. W. Linder, USN
Superintendent

Jack Borsting
Provost

The transonic equation represents an important problem in Gas Dynamics.

This work is relevant to AE 3043 and to research efforts in transonic flow.

Reproduction of all or part of this report is authorized.

This report was prepared by:

REPORT DOCUMENTATION PAGE		READ INSTRUCTIONS BEFORE COMPLETING FORM
1. REPORT NUMBER NPS-57Zi75011	2. GOVT ACCESSION NO.	3. RECIPIENT'S CATALOG NUMBER
4. TITLE (and Subtitle) AN EXACT SOLUTION TO THE TRANSONIC EQUATION		5. TYPE OF REPORT & PERIOD COVERED
		6. PERFORMING ORG. REPORT NUMBER
7. AUTHOR(s) OSCAR BIBLARZ		8. CONTRACT OR GRANT NUMBER(s)
9. PERFORMING ORGANIZATION NAME AND ADDRESS NAVAL POSTGRADUATE SCHOOL MONTEREY, CA 93940		10. PROGRAM ELEMENT, PROJECT, TASK AREA & WORK UNIT NUMBERS
11. CONTROLLING OFFICE NAME AND ADDRESS NAVAL POSTGRADUATE SCHOOL MONTEREY, CA 93940		12. REPORT DATE April 1975
		13. NUMBER OF PAGES 24
14. MONITORING AGENCY NAME & ADDRESS (if different from Controlling Office)		15. SECURITY CLASS. (of this report) UNCLASSIFIED
		15a. DECLASSIFICATION/DOWNGRADING SCHEDULE
16. DISTRIBUTION STATEMENT (of this Report) Approved for public release; distribution unlimited		
17. DISTRIBUTION STATEMENT (of the abstract entered in Block 20, if different from Report) Approved for public release; distribution unlimited		
18. SUPPLEMENTARY NOTES		
19. KEY WORDS (Continue on reverse side if necessary and identify by block number)		
20. ABSTRACT (Continue on reverse side if necessary and identify by block number) The small disturbance equation of transonic flow is solved by a separation of variables technique. The resulting ordinary, nonlinear differential equations are studied in the phase plane where the general solution represents the behavior of the perturbation velocities. In the phase plane, the character of transonic flow is evident. An asymptotic explicit solution is given which encompasses the sonic flow solution. Numerical integration results for the implicit equations are presented and two flows are examined which are intrinsic to the form of the solution.		

TABLE OF CONTENTS

I.	INTRODUCTION	1
II.	SEPARATION OF VARIABLES	2
III.	PHASE PLANE	4
IV.	IMPLICIT SOLUTIONS	11
V.	INTRINSIC FLOWS	14
VI.	CONCLUSIONS	21
VII.	ACKNOWLEDGEMENTS	21
VIII.	REFERENCES	22

LIST OF FIGURES

FIGURE 1.	PHASE PLANE REPRESENTATION	5
FIGURE 2.	PERTURBATION VELOCITIES IN PHASE PLANE	7
FIGURE 3.	Q-Y TRAJECTORIES, y INCREASING	9
FIGURE 4.	P-X TRAJECTORIES, x INCREASING	10
FIGURE 5.	NUMERICAL INTEGRATION OF EQUATION 33	15
FIGURE 6.	NUMERICAL INTEGRATION OF EQUATION 34, $Q \neq 0$	16
FIGURE 7.	INTRINSIC FLOW, SUBSONIC INITIALLY	19
FIGURE 8.	INTRINSIC FLOW, SUPERSONIC INITIALLY REGION I	20

I. INTRODUCTION

With much renewed interest in transonic flow, the limitations of present methods of analysis become evident. The hodograph transformation can be useful only for flows past a small class of airfoils; numerical methods are powerful but lack some generality. It is, therefore, worthwhile to examine anew the possibility and suitability of exact solutions to the two-dimensional, small disturbance potential equation of transonic flow. This equation retains one non-linear term which is essential for non-divergent solutions at Mach one, but the non-linear partial differential equation has proven to be difficult to solve. This inherent difficulty, coupled with the presence of shocks in the flow which cause boundary layer separation, has resulted in the creation of many approximate methods of solution¹ which are employed in the design of transonic airfoils and the like.

Some exact solutions are available for the transonic equation which are not obtained through the hodograph method. Mayer² obtained a solution for the flow in a deLaval nozzle in the form of a series expansion; Goertler and Guderley² report on an exact solution to the "parallel sonic jet." Exact solutions are limited either by boundary conditions as in the hodograph method or by the inherent approximations of the transonic equation. These solutions, however, can be very useful in checking results from approximations to the equation and do represent a practical class of geometries in their own right.

In this paper an exact solution is presented which satisfies the full form of the transonic flow equation and involves 5 parameters. This solution has been obtained through a separation of variables which is appropriate to a re-arranged form of the original equation. These results can be studied in the phase plane where significant features of the transonic equation are evident. The implicit form of the solution can be given an explicit asymptotic form which is both simple and useful. The separated solutions can be manipulated to generate transonic, shockless flows.

II. SEPARATION OF VARIABLES

The transonic equation in two dimensions is³

$$(1-M_\infty^2)\varphi_{xx} + \varphi_{yy} = M_\infty^2(\gamma+1)\varphi_x\varphi_{xx} \quad (1)$$

where

$$\varphi_x = \frac{u}{U_\infty} \text{ and } \varphi_y = \frac{v}{U_\infty}$$

u and v are the perturbation velocities corresponding to the x and y axis respectively, and M_∞ is the Mach number of the unperturbed flow at U_∞ moving in the positive x direction. The coordinates are dimensionless.

Equation 1 can be separated with

$$\tilde{\varphi}(x,y) = X(x)Y(y) + (1-M_\infty^2)x \quad (2)$$

where

$$\tilde{\varphi}(x,y) \equiv M_\infty^2(1+\gamma)\varphi \quad (3)$$

the resulting form is

$$\frac{X'X''}{X} = \frac{Y''}{Y^2} = -\lambda \quad (\lambda > 0)$$

where λ is a separation constant the sign of which is chosen so that Y remains finite as y goes to infinity. In the subsonic wavy wall solution³ it is shown that the separation constant is related to the "wavelength" of the sinusoidal wall. We arrive then at two ordinary, nonlinear equations

$$X'X'' + \lambda X = 0 \quad (4a)$$

$$Y'' + \lambda Y^2 = 0 \quad (4b)$$

To obtain the $X(x)$ solution, let $P(x) = X'$; integrating once we obtain

$$P(x) = \sqrt[3]{-\frac{3}{2}\lambda X^2 + \alpha} \quad (5)$$

where α is a constant of integration. Now, integrating again we get

$$x = x_0 + \int_{x_0}^x \frac{dz}{\sqrt{-\frac{3}{2}\lambda z^2 + \alpha}} \quad (6)$$

which is an implicit form for the solution. The $Y(y)$ solution follows in a similar fashion; letting $Q(y) = Y'$ we arrive at

$$Q(y) = \pm \sqrt{-\frac{2}{3}\lambda Y^3 + \beta} \quad (7)$$

where β is an integration constant. Upon integrating again the result is

$$y = y_0 + \int_{y_0}^y \frac{dW}{\sqrt{-\frac{2}{3}\lambda W^3 + \beta}} \quad (8)$$

which represents the implicit solution for $Y(y)$.

We shall study next the separated solutions in the phase plane before further considerations of the above integrals are given.

III. PHASE PLANE

Since the independent variable does not appear in Eqs. 4a and 4b, then the analysis in the phase plane is appropriate^{4,5}. Using the previous definitions for P and Q we can rewrite Eqs. 5 and 7 as

$$\frac{1}{3}P^3 + \frac{1}{2}\lambda X^2 = \pm \alpha/3 \quad (9)$$

and
$$\frac{1}{2}Q^2 + \frac{1}{3}\lambda Y^3 = \pm \beta/2 \quad (10)$$

Provided that neither α nor β are zero, it is useful at this point to divide Eqs. 9 and 10 by α and β respectively. What results is an equation of the form

$$a^3 + b^2 = \pm 1 \quad (11)$$

where
$$a = \frac{P}{\alpha^{1/3}} \text{ or } \left(\frac{2}{3} \frac{\lambda}{\beta}\right)^{1/3} Y \quad (12)$$

and
$$b = \left(\frac{3}{2} \frac{\lambda}{\alpha}\right)^{1/2} X \text{ or } \frac{Q}{\beta^{1/2}} \quad (13)$$

It is a simple matter to plot Eq. 11 on the phase plane and this is shown in Fig. 1. In this figure, we have also shown the corresponding curves for a circle (a degenerate ellipse), and for a hyperbola. Since both the ellipse and the hyperbola represent solutions to linear equations, the non-linear character of the present solution is evident in Fig. 1.

In order to further explore the features of the phase plane, let us return to the velocity potential; from Eq. 2,

$$\tilde{\varphi}_x = X'Y + (1-M_\infty^2) \quad (14)$$

and
$$\tilde{\varphi}_y = XY' \quad (15)$$

where
$$\tilde{\varphi}_x = \frac{u}{U_\infty M_\infty^2 (1+\gamma)} \quad \text{and} \quad \tilde{\varphi}_y = \frac{v}{U_\infty M_\infty^2 (1+\gamma)}$$

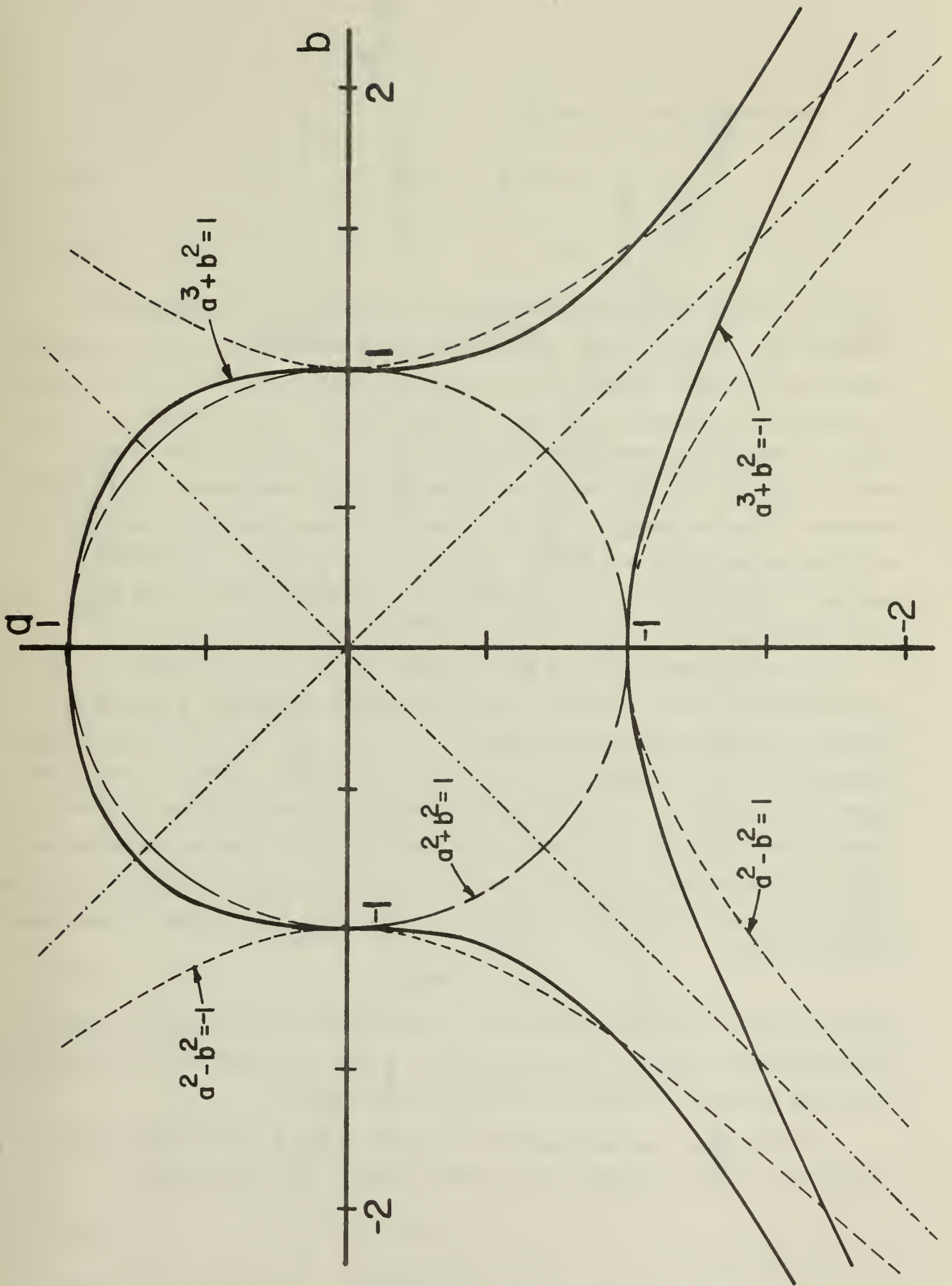


FIGURE 1. PHASE PLANE REPRESENTATION

Rearranging Eqs. 14 and 15

$$X'Y = \tilde{\varphi}_x - (1-M_\infty^2) \quad (16)$$

$$XY' = \tilde{\varphi}_y \quad (17)$$

Clearly, a phase plane representation of X' (or P) vs X corresponds to plotting $[\tilde{\varphi}_x - (1-M_\infty^2)]$ vs $\tilde{\varphi}_y$ with a constant y coordinate. What is equally significant is that the same figure results if we plot Y vs Y' (or Q) along a constant x coordinate. The above inference can be seen from Eqs. 11-13. Figure 2 shows the phase plane in $\tilde{\varphi}_x$ and $\tilde{\varphi}_y$; Z signifies either Y or X' and W signifies either Y' or X depending on which coordinate is being held constant. The character of Fig. 2 is useful because our inquiries as to equilibrium and stability points in the phase plane will have direct physical significance. We shall also find that trajectories will be of some interest.

It can be seen in Fig. 2 that, except for $M_\infty = 1$, the curves do not go through the origin. Since we know that there must exist a region for which no velocity perturbations exist (i.e. $\varphi_x = \varphi_y = 0$), it is clear that intercepts in the ordinate are proportional to $1-M_\infty^2$. That is, the upper curve must correspond to an initially supersonic flow ($1-M_\infty^2 < 0$) and the lower curve to an initially subsonic flow; the axis is the no perturbation point. Although shocks are not necessarily normal but must satisfy the transonic shock polar, the above argument is consistent with normal shocks near Mach one where

$$M_{\infty 1}^2 - 1 = 1 - M_{\infty 2}^2 \quad (18)$$

holds between supersonic (subscript 1) and subsonic Mach numbers. Clearly, without perturbations, a flow may shock and this corresponds to a trajectory along the ordinate between the upper and lower curves.

At this point we are ready to interpret α and β since their sign governs the choice of curve in the phase plane. It follows that

$$\pm \alpha = C_1 (M_\infty^2 - 1) \quad (19)$$

$$\text{and} \quad \pm \beta = C_2 (M_\infty^2 - 1) \quad (20)$$

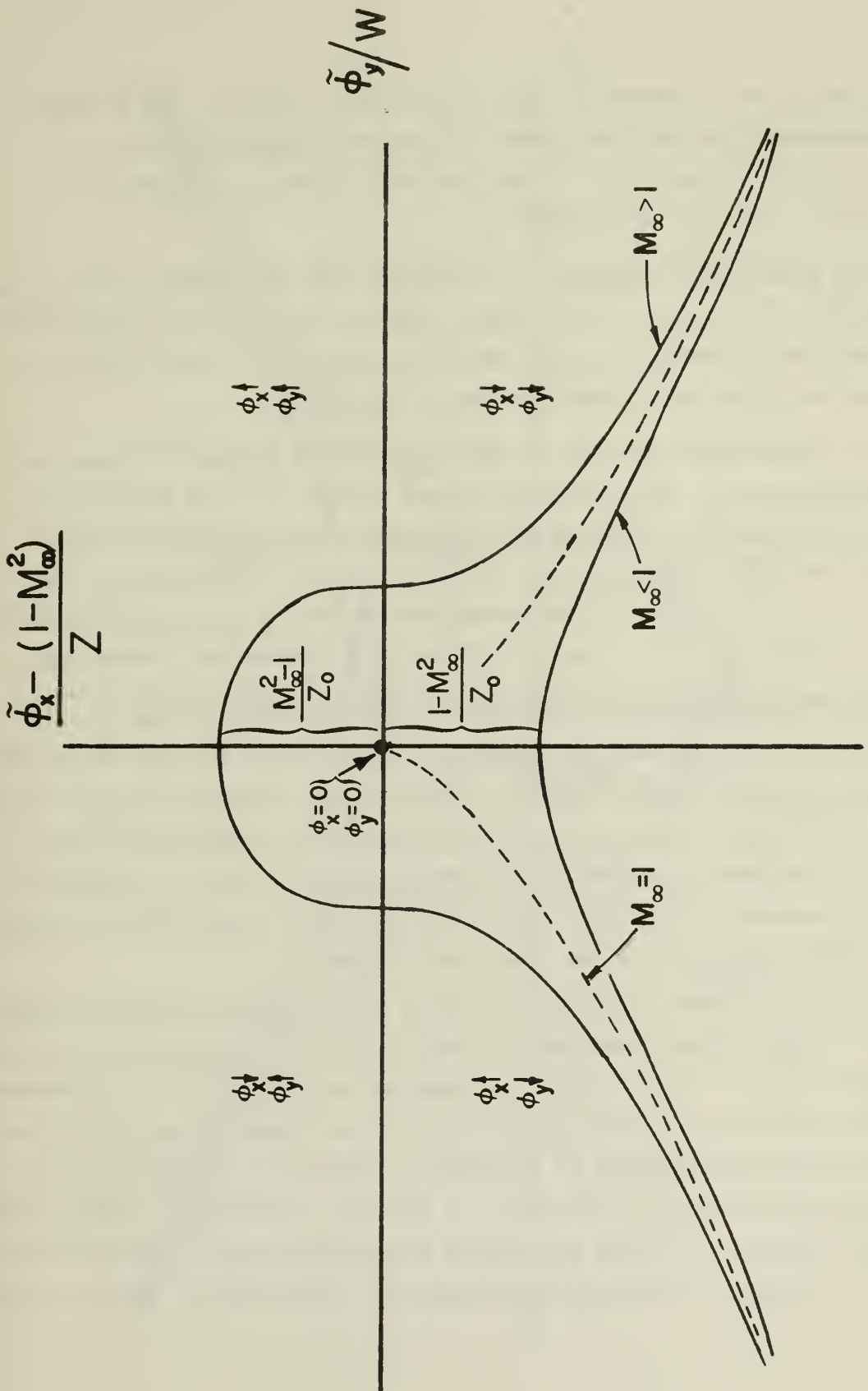


FIGURE 2. PERTURBATION VELOCITIES IN PHASE PLANE

where C_1 and C_2 are constants. The form of Eqs. 19 and 20 can be shown to be consistent with the von Karman's transonic similarity rule as given by Spreiter³ (where for a fixed value of x and y , $X'Y$ must be a function of $(1-M_\infty^2)$, see Section V).

Using phase-plane arguments* it follows that the origin in Fig. 2 is an equilibrium point for $M_\infty=1$. This means that, at least for two dimensions, such a flow cannot develop any perturbations since for P and X equal to zero there is no way the curves may leave the origin.

It is instructive to look at the trajectories in the P - X plane and Q - Y plane separately. The latter are shown in Fig. 3. The arrows indicate the direction of increasing y . The origin is an equilibrium point ($Q'=0$ and $Y'=0$) which implies that the only "stable" trajectory is that for $M_\infty=1$. $Q=0$ corresponds to an asymptote because $y \rightarrow \infty$ as $Q \rightarrow 0$ from above and $y \rightarrow -\infty$ as $Q \rightarrow 0$ from below; however, Q always decreases for increasing y .

The P - X trajectories are more complicated as shown in Fig. 4. The trajectories for $P>0$ and $P<0$ are opposite implying that the $P=0$ intercepts are "singular" points; note, however, that these are points at $x=\pm\infty$. The subsonic side (lower curve) can be traversed without difficulty but the supersonic side shows problems in going from region I ($P<0$) to region II ($P>0$) and viceversa. This difficulty will be easily understood in Section IV where curves are shown in the coordinate plane.

The P - X plane shows trajectories which may elucidate transonic shock behavior. In Fig. 2 the perturbation velocities are indicated for the motion represented by Fig. 4 (i.e. with x increasing) and for $Q > 0$. A supersonic flow would start at the ordinate intercept of the upper curve ($\varphi_x = \varphi_y = 0$) and move to the right whereas an originally subsonic flow would begin at the lower intercept and move to the left. A variety of flows are possible depending on the choice of the free parameters involved; however, the choice is restricted to region II for initially supersonic flow until we introduce transonic

*The equation in $X(x)$ must be modified as follows

$$\text{let } R = \frac{1}{2} (X')^2$$

$$\text{then } X' = \sqrt{2R} \quad \text{and } R' = -\lambda X$$

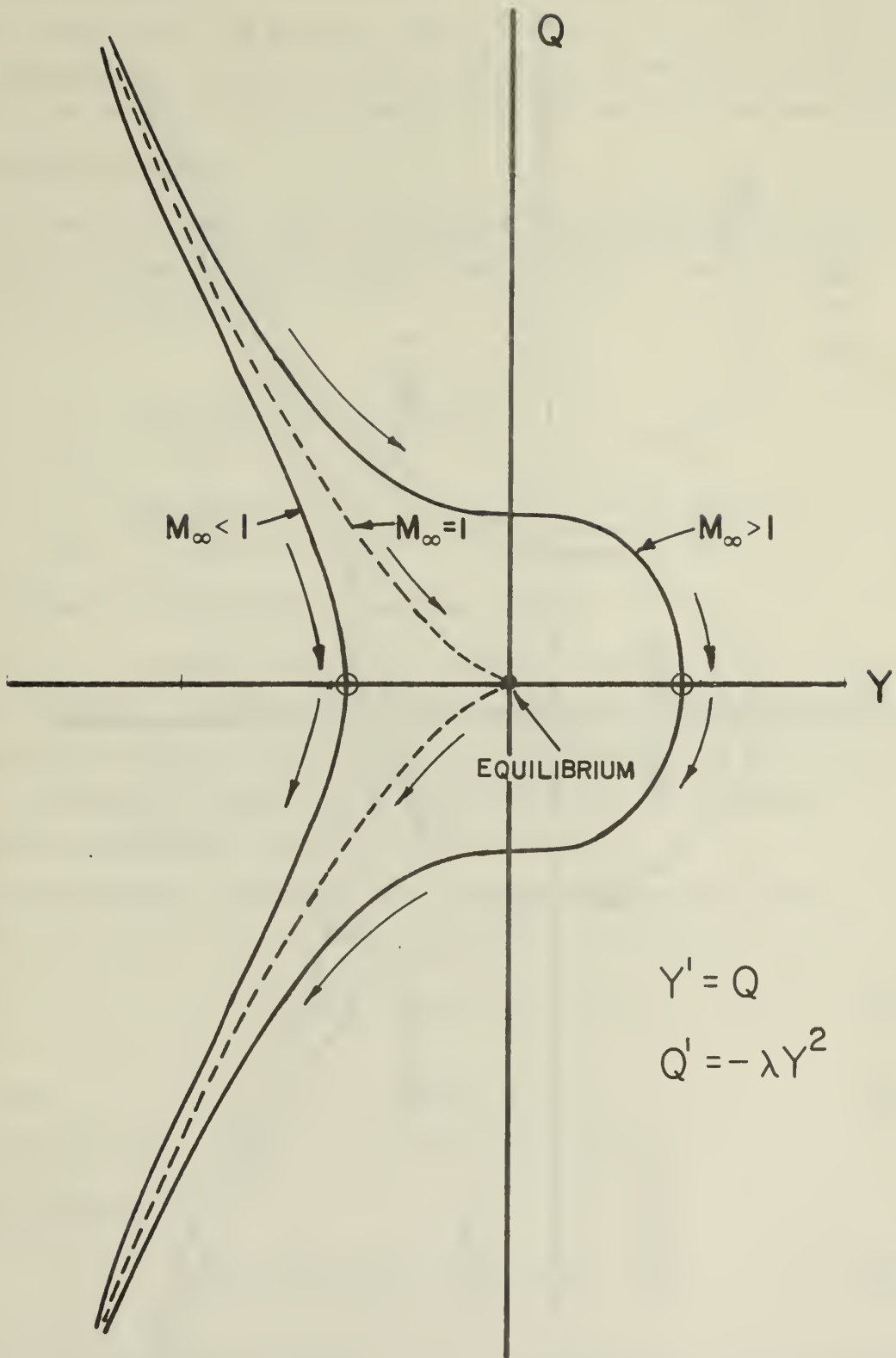


FIGURE 3. Q-Y TRAJECTORIES, y INCREASING

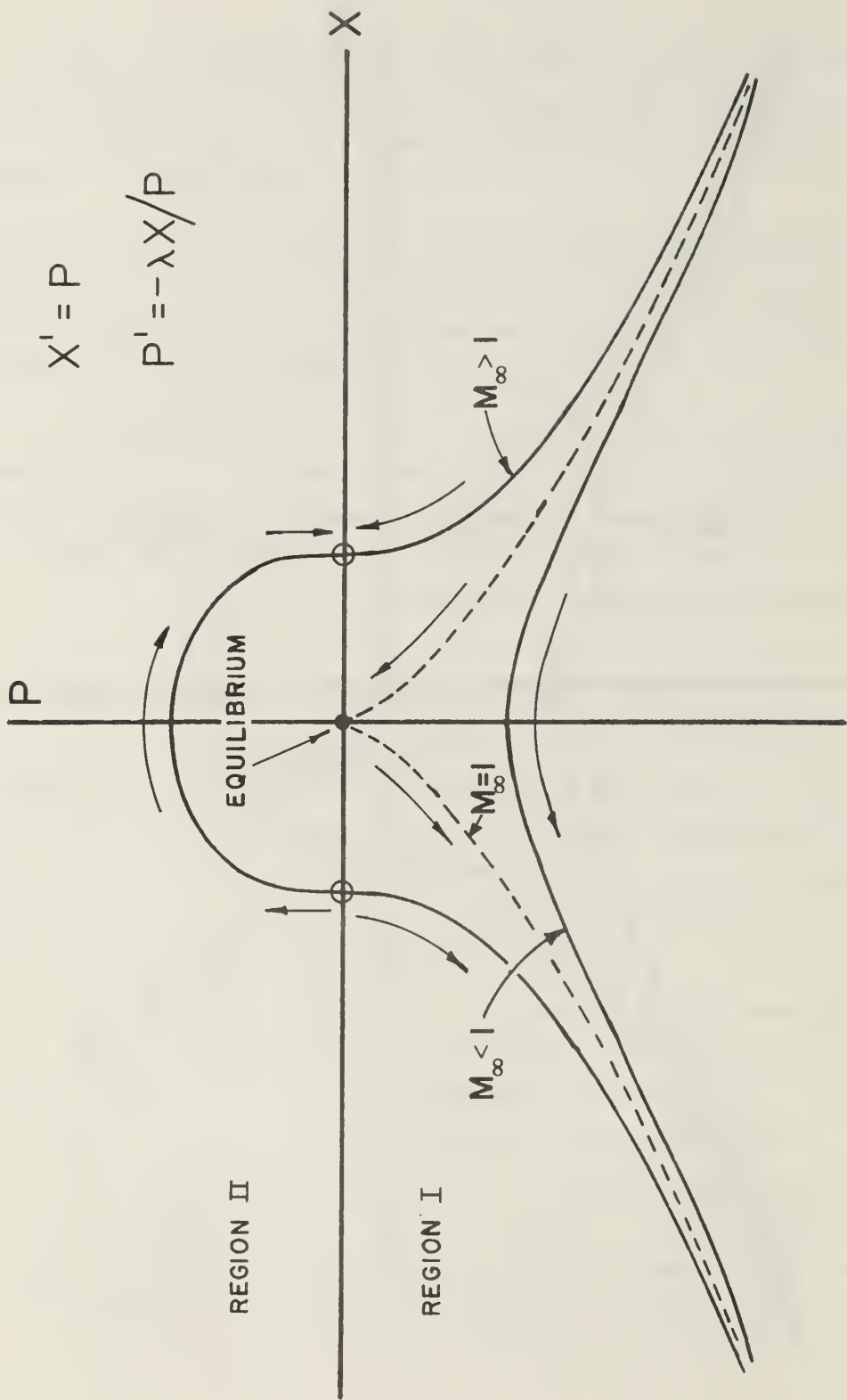


FIGURE 4. P-X TRAJECTORIES, x INCREASING

shocks. The discussion of a subsonic flow which goes through a local supersonic zone within the airfoil appears to be more complicated and will not be attempted here. The important question as to whether or not shocks can be avoided in transonic flow remains to be shown with the phase plane analysis.

IV. IMPLICIT SOLUTIONS

In order to present further discussion of the implicit solutions, we note that for appropriately large values of X and Y the following simplifications take place:

$$P(x) = \sqrt[3]{-\frac{3}{2}\lambda X^2 + \alpha} \cong -\left(\frac{3}{2}\lambda\right)^{1/3} X^{2/3} \quad X > \left(\frac{2\alpha}{3\lambda}\right)^{1/2}$$

and

$$Q(y) = \sqrt{-\frac{2}{3}\lambda Y^3 + \beta} \cong -\left(\frac{2}{3}\lambda\right)^{1/2} Y^{3/2} \quad Y < -\left(\frac{3\beta}{2\lambda}\right)^{1/2}$$

where only positive values of Q have been chosen.

This is, of course, evident from Figs. 1-4 where it can be seen that the subsonic and supersonic branches approach a common asymptote so that at sufficiently high values there is no distinction between the subsonic and supersonic regimes within transonic flow. The approximation, furthermore, represents the exact solution for $M_\infty=1$.

Under the above conditions, the integrals represented by Eqs. 6 and 8 become

$$X = -\frac{\lambda}{18} x^3 \quad (21)$$

and

$$Y = -\frac{6}{\lambda} (y-y_0)^{-2} \quad (22)$$

(Note that $Y = -\infty$ at $y = y_0$, whereas $X=0$ at $x=0$)

Therefore, from Eq. 2,

$$\tilde{\varphi}(x,y) = \frac{1}{3} \frac{x^3}{(y-y_0)^2} + (1-M_\infty^2)x \quad (23)$$

where, λ , the separation constant related to a geometry input has dropped out. The limit represented by Eqs. 21 and 22 is suggestive of supersonic flow at regions away from the body surface. Consider the perturbation velocities,

$$\tilde{\varphi}_x = \frac{x^2}{(y-y_0)^2} + (1-M_\infty^2) \quad (24)$$

and
$$\tilde{\varphi}_y = -\frac{2}{3} \frac{x^3}{(y-y_0)^3} \quad (25)$$

If we "force" the characteristics for supersonic flow on these results, we find that, using $x = \pm (M_\infty^2 - 1)^{\frac{1}{2}} (y - y_0)$, Eqs. 24 and 25 become

$$\tilde{\varphi}_x = 0 \quad (26)$$

$$\tilde{\varphi}_y = \mp \frac{2}{3} (M_\infty^2 - 1)^{3/2} \quad (27)$$

It is interesting to compare these results with a Prandtl-Meyer expansion for values close to the sonic line. The first non-zero term of the angle ν (which changes $M=1$ to $M_\infty > 1$) is ⁶, using a series expansion for the \tan^{-1} ,

$$\nu = \frac{2}{3} \frac{(M_\infty^2 - 1)^{3/2}}{(\gamma + 1)} + \dots \quad (28)$$

but from Eqs. 26, 27, and 3

$$\nu \cong \tan \nu = \frac{v}{U_\infty + u} = \frac{2}{3} \frac{(M_\infty^2 - 1)^{3/2}}{(\gamma + 1) M_\infty^2} \quad (29)$$

The comparison is good since M_∞ must be close to 1. If M_∞ is exactly one, then we know that $\nu = 0$; the sonic solution is simply

$$\tilde{\varphi}(x, y) = \frac{1}{3} \frac{x^3}{(y - y_0)^2} \quad (30)$$

It is evident that if x is zero φ_x , φ_{xx} , and φ_{yy} will all be zero which corresponds to the trivial solution to the transonic equation. This is the equilibrium point alluded to in the previous Section.

The parallel sonic jet solution of Goertler and Guderley² is comprised of Eqs. 8 and 21, but note that sign of λ as chosen by these authors is opposite that used in this work. The result is to make their $Y(y)$ go to infinity at some finite y , and this appears to be inconsistent with the

character of unbounded flow. As will be shown at the end of this Section, our $Y(y)$ has an upper limit as y goes to infinity. It is possible, however, to obtain Eq. 30 from the Goertler and Guderley solution.

Before proceeding to depict the entire range of the integrals given by Eqs. 6 and 8, it is worthwhile to examine their behavior near $X=0$ and $Y=0$. We have, using Eqs. 19 and 20 as well,

$$P \cong \pm \alpha^{1/3} = C_1^{1/3} (M_\infty^2 - 1)^{1/3} \quad (31)$$

which says that the slope of X near the origin is constant, positive for supersonic flow and negative for subsonic flow. In the y direction we have

$$\pm Q \cong \beta^{1/2} = C_2^{1/2} (M_\infty - 1)^{1/2} \quad (32)$$

which implies that only the supersonic flow solution crosses the abscissa and with a positive, constant slope. Because of the third power on Y , the straight line portion of it will be conspicuous.

If we now write Eqs. 6 and 8 for $M_\infty \neq 1$ as

$$x = - \left(\frac{2}{3\lambda}\right)^{1/2} \alpha^{1/6} \int_0^{\tilde{x}} \frac{dz}{\sqrt[3]{z^2 + 1}} \quad (33)$$

$$y - y_0 = \pm \left(\frac{3}{2\lambda}\right)^{1/3} \beta^{-1/6} \int_{-\tilde{y}}^{\infty} \frac{dw}{\sqrt{w^3 + 1}} \quad (34)$$

and define

$$\tilde{x} \equiv x \alpha^{-1/6} \left(\frac{3\lambda}{2}\right)^{1/2} \quad (35)$$

$$(\tilde{y} - \tilde{y}_0) \equiv (y - y_0) \beta^{1/6} \left(\frac{2\lambda}{3}\right)^{1/3} \quad (36)$$

then we can plot \tilde{X} vs \tilde{X} and \tilde{Y} vs $(\tilde{y}-\tilde{y}_0)$. This is shown in Figs. 5 and 6. These results were obtained by numerical integration of the equations. In Figure 5, the axis was chosen as the point of symmetry since the curves go to infinity. It is clear that the supersonic solutions of region I cannot pass into region II (except at $\pm\infty$) as implied by the phase plane plot, Fig. 4. The subsonic solution has no discontinuities. For values of X greater than ± 10 , the form of Eq. 21 well represents the curves within three significant figures. In Fig. 6 we have plotted only the curves for $Q \geq 0$; the curves for $Q \leq 0$ would correspond to a reflection of the shown curves about the ordinate. Since Q always decreases with increasing y , crossing the abscissa in Fig. 3 requires a trajectory going through infinity. It is clear in Fig. 6 that only the supersonic solution crosses the y -axis (at $\tilde{y}-\tilde{y}_0 = + 2.8$) and that it is asymptotic to $\tilde{Y}=1.0$; similarly the subsonic solution is asymptotic to $\tilde{Y}=-1.0$. For values of \tilde{Y} less than -5 the curves are well represented by Eq. 22. With knowledge of $X(x)$ and $Y(y)$, P and Q can be found from Eqs. 5 and 7 respectively.

V. INTRINSIC FLOWS

The solutions which arise from separation of variables in the transonic equation generate three flows which we shall call intrinsic. The reasoning will be evident in the arguments shown below. Eqs. 33 and 34 may be written as ($M_\infty \neq 1$)

$$d\tilde{x} = \frac{d\tilde{X}}{3\sqrt{-\tilde{X}^2 \pm 1}} \quad (37)$$

and

$$d\tilde{y} = \frac{\pm d\tilde{Y}}{2\sqrt{-\tilde{Y}^3 \pm 1}} \quad (38)$$

Now at the body surface $y_b = f(x)$ or

$$\tilde{Y}_b = g(\tilde{X}) \quad (39)$$

Let us define the intrinsic flows as ones for which

$$\tilde{Y}_b^3 = -\tilde{X}^2 \pm 1 \quad (40)$$

It is not difficult to show that as a result of Eq. 40, taking derivatives,

$$\frac{\pm d\tilde{Y}_b}{\sqrt{-\tilde{Y}_b^3 \pm 1}} = -\frac{2}{3} \frac{d\tilde{X}}{[-\tilde{X}^2 \pm 1]^{2/3}} \quad (41)$$

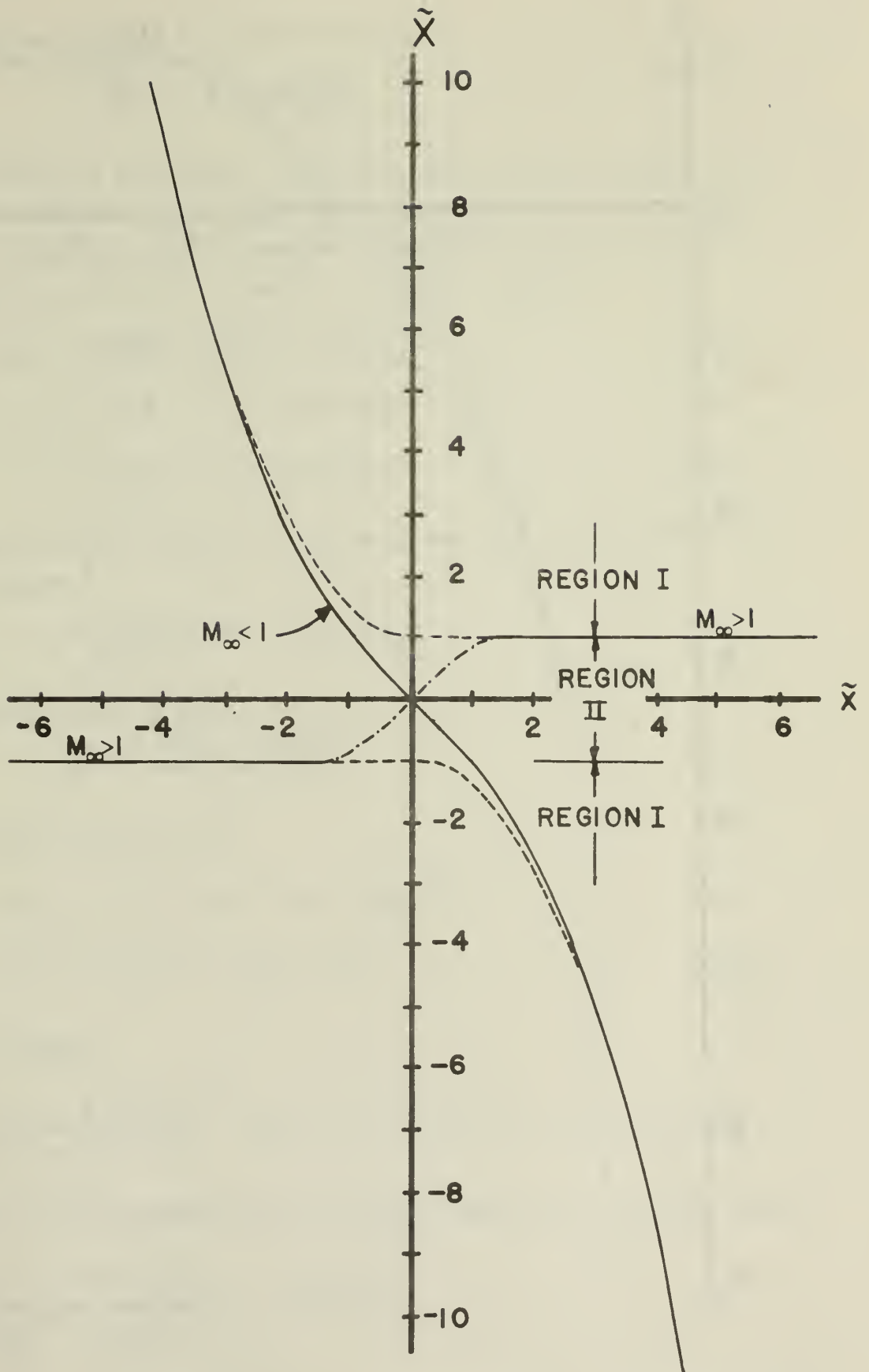


FIGURE 5. NUMERICAL INTEGRATION OF EQUATION 33

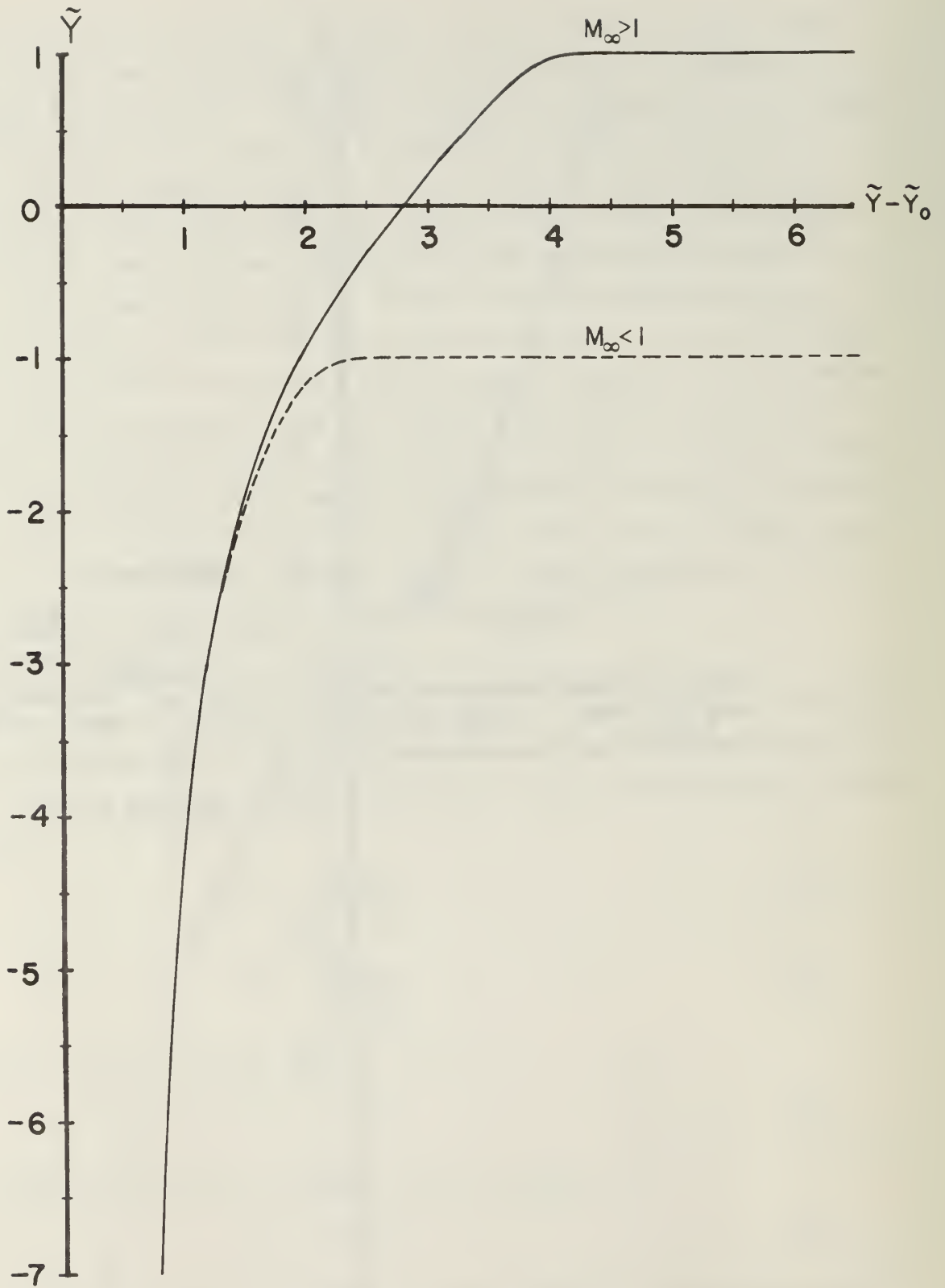


FIGURE 6. NUMERICAL INTEGRATION OF EQUATION 34, $Q \geq 0$

Introducing Eqs. 37 and 38, the above becomes

$$\frac{d\tilde{y}_b}{d\tilde{x}} = -\frac{2}{3} \frac{1}{\sqrt[3]{-\tilde{x}^2+1}} \quad (42)$$

Since, according to Figs 4 and 5, there are three distinct curves (one subsonic and two supersonic) we would anticipate that Eq. 42 represents three flows. Before going to a numerical integration, let us see what Eq. 42 yields for both the $\tilde{X} > 1$ and $\tilde{X} < 1$ limits. We have

$$\tilde{y}_b = \text{constant} - 6/\tilde{x} \quad \text{for } \tilde{X} > 1 \quad (43)$$

$$\text{and } \tilde{y}_b = \begin{cases} -\frac{2}{3} \tilde{x}, & \tilde{X} < 1 \text{ supersonic} \\ +\frac{2}{3} \tilde{x}, & \tilde{X} < 1 \text{ subsonic} \end{cases} \quad (44a)$$

$$(44b)$$

Now the pressure coefficient in two-dimensional flow at the surface can be found as follows ³

$$C_p = \frac{P - P_\infty}{\frac{1}{2} \rho_\infty U_\infty^2} = -2 \phi_x(x, y_b) \quad (45)$$

But, according to Eqs 3 and 14

$$C_p = -\frac{2[X'Y_b + (1-M_\infty^2)]}{M_\infty^2(1+\gamma)} \quad (46)$$

It can further be shown that

$$X'Y_b = [-\tilde{X}^2+1]^{2/3} (\alpha^{1/3}) \left(\frac{3\beta}{2\lambda}\right)^{1/3} \quad (47)$$

$$\text{where } (\alpha\beta)^{1/3} = (C_1 C_2)^{1/3} (M_\infty^2 - 1)^{2/3} \quad (48)$$

So that C_p becomes

$$C_p = -\frac{2}{M_\infty^2(1+\gamma)} \left\{ \left(\frac{3C_1 C_2}{2\lambda}\right)^{1/3} (M_\infty^2 - 1)^{2/3} [-\tilde{X}^2+1]^{2/3} + (1-M_\infty^2) \right\} \quad (49)$$

Eq. 49 shows the dependance of C_p on $(1-M_\infty^2)$ explicitly. We next define

$$\tilde{C}_p \equiv \frac{C_p M_\infty^2(1+\gamma) + 2(1-M_\infty^2)}{2 \left(\frac{3C_1 C_2}{2\lambda}\right)^{1/3} (M_\infty^2 - 1)^{2/3}} = -[-\tilde{X}^2+1]^{2/3} \quad (50)$$

where \tilde{C}_p is the part of the pressure coefficient which varies with the coordinate of the surface.

Of the three possible flows, only two turn out to be reasonable, namely, the one corresponding to $M_\infty < 1$ and that for $M_\infty > 1$, region I. These flows are shown in Figs 7 and 8 where \tilde{y}_b and \tilde{C}_p are plotted as a function of \tilde{x} . The initially subsonic flow represented in Fig. 7 corresponds to a concave shape connected to a convex one through a straight section; there is no stagnation point. The curvature of \tilde{C}_p reflects the concave-convex features of the surface. The maximum value of \tilde{C}_p is minus one at $\tilde{x} = 0$. We note that, since $M_\infty < 1$, the conventional C_p will always be negative unless λ itself is not as previously defined. The initially supersonic flow shown in Fig. 8 is to be interpreted as flow in the minus x and minus y directions (i.e., to the left and down). Here the shape is all concave and we expect few differences between this flow and the previous one. \tilde{C}_p , for example, goes to zero at $\tilde{x} = 0$ where one would anticipate noticeable differences as evidenced in Fig. 5. These results will, of course, break down at some \tilde{y}_b where the small perturbation assumptions begin to be exceeded. These two flows emerge in a straightforward way from the form of the separated solutions and should become part of the important class of transonic flows.

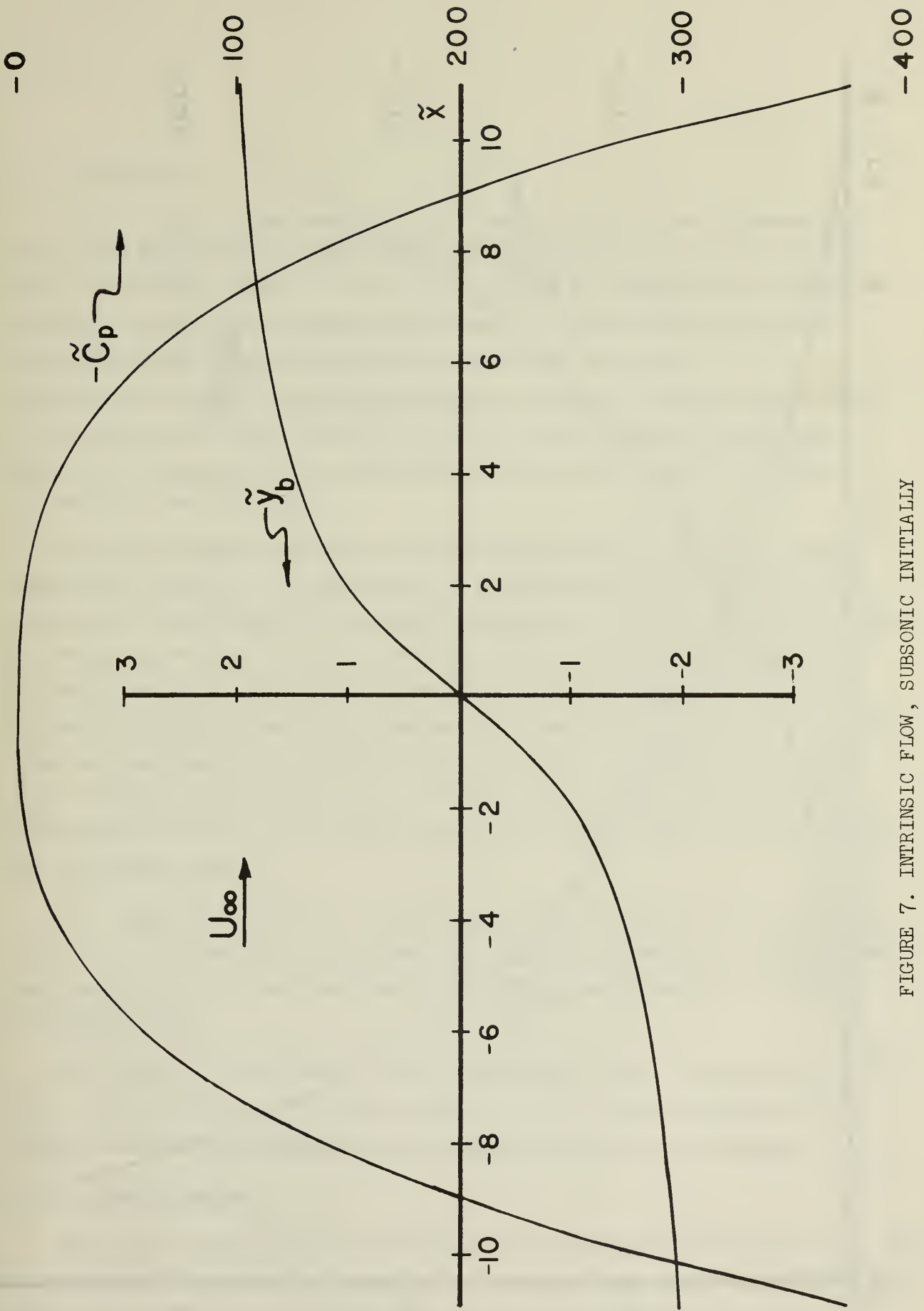


FIGURE 7. INTRINSIC FLOW, SUBSONIC INITIALLY

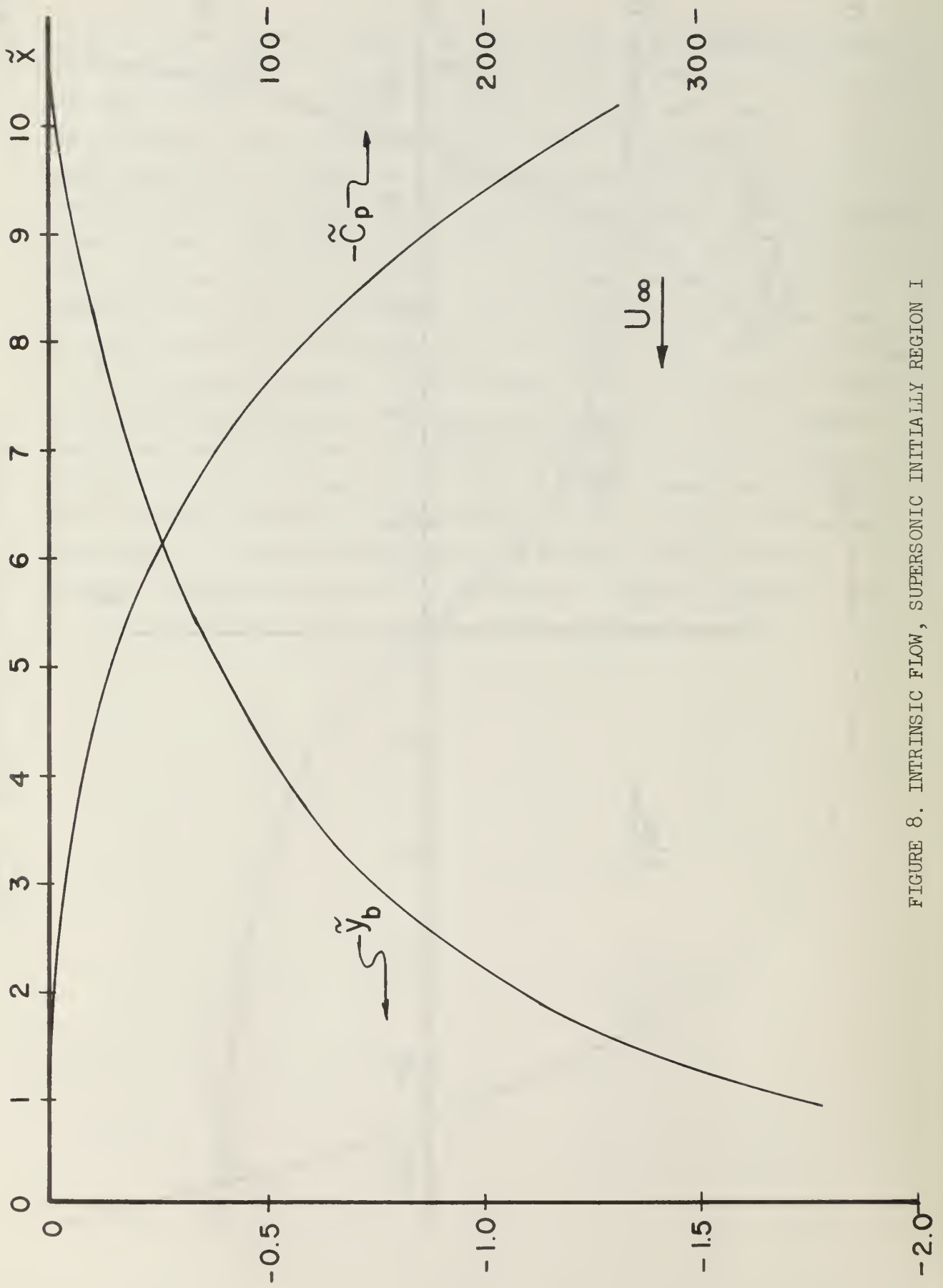


FIGURE 8. INTRINSIC FLOW, SUPERSONIC INITIALLY REGION I

VI. CONCLUSIONS

The utility of the exact solution shown in this paper is associated with cases where the boundary conditions are compatible with the separation of variables scheme. This is particularly significant on the body surface (the so-called tangency condition); a family of flows which is intrinsic to the form of the solutions has been discussed. At infinity, the perturbation must be finite or zero and the fact that $Y(y)$ is bounded as $y \rightarrow \infty$ means that this boundary condition may be handled as well. Of course, there is a class of internal flow problems for which our solution may also apply.

Since the phase plot may be interpreted in terms of the perturbation velocities φ_x and φ_y , we have before us a fundamental tool for studying the general properties of the transonic equation. Paths of constant x or y coordinate are easy to see in practice and one can find trajectories for which the perturbation velocities will remain constant. The allowed trajectories with increasing x promise to be particularly useful in uncovering the behavior of shocks in transonic flow. Moreover, the conclusions from the phase plane that govern sonic flow point out some rather fundamental behavior of two-dimensional flow, namely, that sonic flow is an equilibrium point.

The asymptotic solution to the velocity potential has been identified with sonic flow and with a very weak Prandtl-Meyer expansion. Certainly, the simplicity of the mathematical form of this result makes it worthy of further study.

The numerical integration results given have aided in explaining some of the features of the given solutions. The characteristics of the flows presented will hopefully have an impact on practical designs.

VII. ACKNOWLEDGEMENTS

The author would like to acknowledge his colleagues, Professor A. E. Fuhs for introducing the problem, and Drs. M. F. Platzer and R. A. Hess for the helpful discussions, all of them from the Naval Postgraduate School.

VIII. REFERENCES

1. P. A. Newman and D. O. Allison, "An Anotated Bibliography on Transonic Flow Theory," NASA TM X-2363, September 1971.
2. K. G. Guderley, The Theory of Transonic Flow, (Pergamon Press, London, 1962) Chap. IV.
3. H. W. Liepmann and A. Roshko, Elements of Gasdynamics, (John Wiley and Sons, Inc., New York, 1957) Chaps. 8, 10, and 11.
4. R. A. Struble, Nonlinear Differential Equations, (McGraw-Hill Inc, New York, 1962).
5. N. Minorsky, Introduction to Non-Linear Mechanics, (J. W. Edwards, Ann Arbor, 1947).
6. A. E. Bryson, "An Experimental Investigation of Transonic Flow Past Two-Dimensional Wedge and Circular-Arc Sections Using a Mach-Zehnder Interferometer," NACA TN2560, November 1951.

DISTRIBUTION LIST

	<u>No. of Copies</u>
1. Defense Documentation Center Cameron Station Alexandria, VA 22314	12
2. Library, Code 0212 Naval Postgraduate School Monterey, CA 93940	2
3. Chairman, Department of Aeronautics Code 57 Naval Postgraduate School Monterey, CA 93940	1
4. Dean of Research Code 023 Naval Postgraduate School Monterey, CA 93940	2
5. Department of Aeronautics Code 57 Naval Postgraduate School Monterey, CA 93940	
Prof. H. W. Burden	1
Prof. D. J. Collins	1
Prof. A. E. Fuhs	1
Dr. M. Clauser	1
Prof. R. A. Hess	1
Prof. M. F. Platzter	1
Prof. R. P. Shreeve	1
Prof. M. H. Vavra	1
Prof. R. D. Zucker	1
6. Prof. Oscar Biblarz Code 57Zi Naval Postgraduate School Monterey, CA 93940	5
7. Stanford University Department of Aeronautics and Astronautics Stanford, CA 94305	
Prof. M. D. van Dyke	1
Prof. W. G. Vincenti	1
Prof. A. E. Bryson	1
Prof. J. R. Spreiter	1

- | | | |
|-----|---|--------|
| 8. | Prof. H. W. Liepmann
GALCIT
California Institute of Technology
Pasadena, CA 91100 | 1 |
| 9. | Prof. J. D. Cole
University of California
at Los Angeles
Department of Engineering
Los Angeles, CA 9007 | 1 |
| 10. | Naval Air Systems Command
Washington, D. C. 20360
Dr. H. J. Mueller, Code AIR310A
Code AIR 320D | 1
1 |
| 11. | U. S. Army Missile Command
Redstone Arsenal, Alabama 35809
Dr. D. J. Spring | 1 |
| 12. | Naval Ship Research and Development Center
Bethesda, Maryland 20034
Dr. Tsge C. Tai | 1 |

U167584

DUDLEY KNOX LIBRARY - RESEARCH REPORTS



5 6853 01058207 5

~~U1675~~